PROCEEDINGS OF SCIENCE

Study of productions of $K_S^0 K_S^0$ (single-tag) and $\eta'\pi^+\pi^-$ (no-tag) in two-photon collisions

Qingnian Xu[∗ †]
Institute of High Energy Physics, Chinese Academy of Siceces
University of Chinese Academy of Sciences
E-mail: xuqingnian10@mails.ucas.ac.cn

A measurement of the cross section for K_S^0 pair production in single-tag two-photon collisions, $\gamma^*\gamma \to K_S^0 K_S^0$, for Q^2 up to 30 GeV^2 is reported. Here Q^2 is the negative of the invariant mass squared of the tagged photon. For the first time, the transition form factor of the $f_2'(1525)$ meson is measured separately for the helicity-0, -1, and -2 components and compared with theoretical calculations. The $\gamma^*\gamma$ partial decay widths of the χ_{c0} and χ_{c2} charmonia are measured as a function of Q^2. The measurements of $\gamma\gamma \to \eta_c(1S), \eta_c(2S) \to \eta'\pi^+\pi^-$ with η' decays to $\gamma\rho$ and $\eta\pi^+\pi^-$ are reported as well. First observation of $\eta_c(2S) \to \eta'\pi^+\pi^-$ with a significance 5.5σ including systematic error is obtained. The products of the two-photon decay width and branching fraction of decays to $\eta'\pi^+\pi^-$ are determined for the $\eta_c(1S)$ and $\eta_c(2S)$, respectively. The cross section for $\gamma\gamma \to \eta'\pi^+\pi^-$ and $\eta' f_2(1270)$) are measured for the first time. These results for the $K_S^0 K_S^0$ ($\eta'\pi^+\pi^-$) production are based on the data sample of 759 fb^{-1} (941 fb^{-1}) collected with the Belle detector at the KEKB asymmetric-energy e^+e^- collider.

39th International Conference on High Energy Physics
4-11 July, 2018
Seoul, Korea

[∗]Speaker.
[†]On behalf of the Belle Collaboration.

PoS(ICHEP2018)677

1. Introduction

A Q^2 dependence of the transition form factor (TFF) of a meson produced by a formation process from two-photon fusion can be measured in the single-tag two-photon processes, where either photon is highly virtual and the other photon regarded as (quasi-) real. The measurements of TFF or the $\gamma^*\gamma$ cross sections are applied for studies of QCD based on models of $q\bar{q}$ mesons [1] and exotic hadrons, and hadron tomography through an extraction of generalized distribution amplitude (GDA)[2]. In addition, the size of the cross sections can be a reference of the Light-by-Light hadronic contribution which is used in a theoretical evaluation of the anomalous magnetic moment of the muon $(g-2)$ [3].

Precise measurement of the $\eta_c(1S)$ and $\eta_c(2S)$ two-photon decay widths may provide sensitive tests for QCD models [4]. CLEO made the first measurement of the $\eta_c(2S)$ two-photon decay width $\Gamma_{\gamma\gamma}$ via $K_S^0 K^+\pi^-$ but observed no signal for the $\eta_c(2S) \to \eta'\pi^+\pi^-$ decay [5]. The cross sections for two-photon production of meson pairs have been predicted in the leading term QCD calculation [6] and the handbag model [7], and measured in the experiments by Belle [8]. There is no specific QCD prediction for the two-photon production of either the pseudoscalar-tensor meson pair $\eta' f_2(1270)$ or the three-body final state $\eta'\pi^+\pi^-$.

The measurements are performed using the Belle detector [9] at the asymmetric e^+e^- collider KEKB [10]. The collision data collected at e^+e^- c.m. energies near the $\Upsilon(4S)$ mass (10.6 GeV), 60 MeV below it, and the $\Upsilon(5S)$ mass (10.9 GeV) are used.

2. Study of $\gamma^*\gamma \to K_s^0 K_s^0$

The $\gamma^*\gamma-$based cross section as a function of W for five Q^2 regions from 3 GeV^2 to 30 GeV^2, in W region below 2.6 GeV, is derived and shown in Figure 1. We find the cross section has peaks near the threshold and the mass of $f_2'(1525)$, but no significant enhancement in the $f_2(1270)/a_2(1320)$ region. The cross section gradually decreases according to Q^2.

Because the peaks from the χ_{c0} and χ_{c2} charmonia are as narrow as the mass resolution of the detector, we evaluate the peak yields with the product of the two-photon decay width $\Gamma_{\gamma^*\gamma}$ and the branching fraction to the final state, instead of the W dependence of the cross section. The experimental results are plotted as a function of Q^2 in Fig. 2 as a ratio to the corresponding zero$-$tag measurement (at $Q^2 = 0$).

We have performed a partial-wave analysis to obtain the TFF of $f_2'(1525)$. The obtained Q^2 dependences of the $f_2'(1525)$ TFFs are plotted in Fig. 3. The curves are the theoretical prediction [1]. They show good agreement for the helicity-0 and -2 states. As for the helicity-1, the prediction is slightly larger, but is not inconsistent.

3. Study of $\gamma\gamma \to \eta'\pi^+\pi^-$

The fit results for the $\eta_c(1S)$ and $\eta_c(2S)$) signals are shown in Fig. 4. The products of the two-photon decay width and branching fraction (B) of decays to $\eta'\pi^+\pi^-$ are determined to be $\Gamma_{\gamma\gamma}B(\eta_c(1S)) = [65.4 \pm 2.6 \text{ (stat)} \pm 6.9 \text{ (syst)}]$ eV and $\Gamma_{\gamma\gamma}B(\eta_c(2S)) = [5.6^{+1.2}_{-1.1} \text{ (stat)} \pm 1.1 \text{ (syst)}]$ eV.

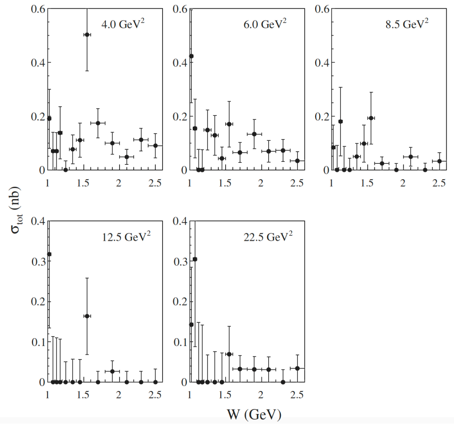

Figure 1: The $\gamma^*\gamma$ based total cross section for $\gamma^*\gamma \to K_S^0K_S^0$ as a function of W for the five Q^2 regions whose central value is shown in the subpanel.

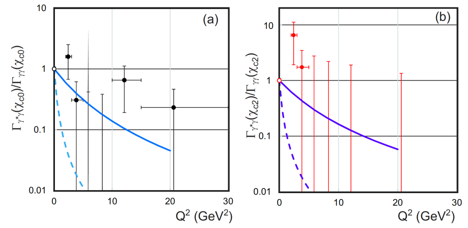

Figure 2: Q^2 dependence of the two-photon decay width of χ_{c0} (left) and χ_{c2} (right) normalized by that for $Q^2 = 0$. Refer to the paper [11].

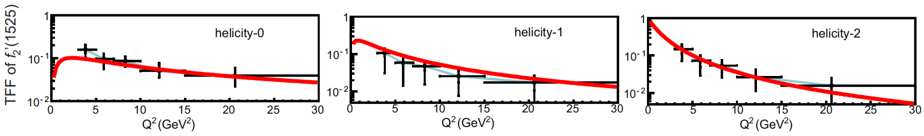

Figure 3: TFFs for the three helicity states of the $f_2'(1525)$ from the present measurement. The gray band shows the normalization error. The curves are from a theoretical prediction [1].

An enhancement near 1960 MeV$/c^2$ is observed in the $\eta_c(1S)$ signal window, but no such excess is seen in the $\eta_c(1S)$ sideband region. We label it the $f_0(2080)$, with mass and spin to be given in study. The fit results for the $f_0(980)$, $f_2(1270)$ and $f_0(2080)$ components are shown in Fig. 5 (a), where the $M_{\pi^+\pi^-}$ distribution is filled with the fitted $\eta_c(1S)$ bin-by-bin yields including the $\eta_c(1S)$ decays to both two-body and three-body final states. Figure 5 (b) shows the distribution of $\cos\theta_{\rm hel}$ for the $f_0(2080)$ candidate events, which are extracted by fitting the $f_0(2080)$ signal in each angular bin, together with MC expectations for $J^{PC} = 0^{++}$ and 2^{++}.

We utilize the data sample selected in the $\eta' \to \eta\pi^+\pi^-$ mode to measure the non-resonant production of $\eta'\pi^+\pi^-$ final states via two-photon collisions. The W-dependent cross sections of the production processes $\gamma\gamma \to \eta' f_2(1270)$ and $\gamma\gamma \to \eta'\pi^+\pi^-$ after subtraction of the $\eta' f_2(1270)$ contribution are measured. The measured differential cross sections in $|\cos\theta^*|$ for $\gamma\gamma \to \eta' f_2(1270)$ show an ascending trend, and its rate of increase is greater in the larger W ranges.

4. summary

For the first time, we find production of the $f_2'(1525)$, $\chi_{c0}(1)$, and $\chi_{c2}(1P)$ mesons in high-Q^2 $\gamma^*\gamma$ scattering[11]. We have measured the χ_{c0} and χ_{c2} partial decay widths $\Gamma_{\gamma^*\gamma}$ as a function of Q^2, as well as the total cross section near the $K_S^0K_S^0$ mass threshold. A partial-wave analysis has been conducted, and the helicity-0, -1, and -2 transition form factors (TFFs) of the $f_2(1525)$ meson are measured. The Q^2 dependence of the above resonances and structures are compared with the

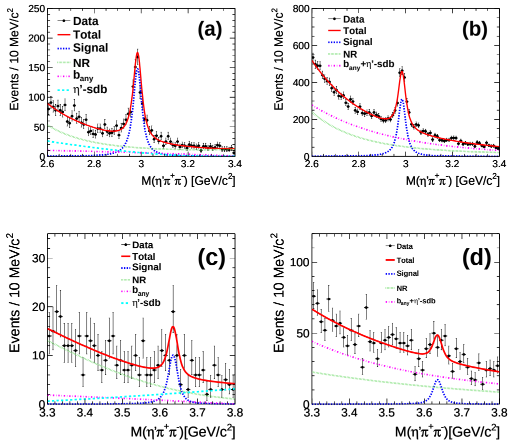

Figure 4: The invariant mass distribution for the $\eta'\pi^+\pi^-$ candidates for (a) [(c)] the $\eta\pi\pi$ mode and (b) [(d)] the $\gamma\rho$ mode, in the $\eta_c(1S)$ [$\eta_c(2S)$] region.

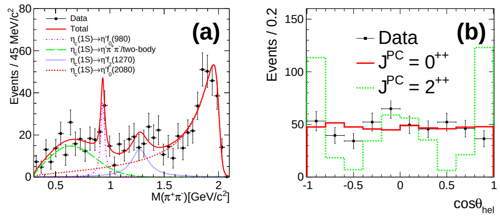

Figure 5: The fit results for the $f_0(980)$, $f_2(1270)$ and $f_0(2080)$ (a) and the distribution of the cosine of helicity angle $\theta_{\rm hel}$ for the $f_0(2080)$ candidate events (b). See the paper [12] in details.

$q\bar{q}$-meson model predictions [1], and the comparisons show that they are not inconsistent for all of them.

The $\eta_c(1S)$, $\eta_c(2S)$ and non-resonant $\eta'\pi^+\pi^-$ production via two-photon collisions is measured [12]. We report the first observations of the signals for $\eta_c(1S)$ decays to $\eta' f_0(2080)$ with $f_0(2080) \to \pi^+\pi^-$ and $\eta_c(2S)$ decays to $\eta'\pi^+\pi^-$, the measured products of the two-photon decay width and the branching fraction for the $\eta_c(1S)$ and $\eta_c(2S)$ decays to $\eta'\pi^+\pi^-$, and the measurement of non-resonant production of two-body $\eta' f_2(1270)$ and three-body $\eta'\pi^+\pi^-$ final states via two-photon collisions.

References

[1] G. A. Schuler, F. A. Berends, and R. van Gulik, Nucl. Phys. B 523, 423 (1998).

[2] S. Kumano, Qin-Tao Song, and O.V. Teryaev, Phys. Rev. D 97, 014020 (2018).

[3] G. Colangelo, M. Hoferichter, B. Kubis, M. Procura and P. Stoffer, Phys. Lett. B 738, 6 (2014).

[4] J. P. Lansberg and T. N. Pham, Phys. Rev. D **74**, 034001 (2006); N. Brambilla, A. Pineda, J. Soto, A. Vairo, Rev. Mod. Phys. **77**, 1423 (2005).

[5] D.M. Asner *et al.* (CLEO Collaboration), Phys. Rev. Lett. **92**, 142001 (2004).

[6] M. Benayoun and V. L. Chernyak, Nucl. Phys. **B329**, 285 (1990).

[7] M. Diehl, P. Kroll and C. Vogt, Phys. Lett. B **532**, 99(2002).

[8] A.J. Bevan, B. Golob, Th. Mannel, S. Prell and B.D. Yabsley, Eds., Eur. Phys. Jour. C **74**, 3026 (2014).

[9] J. Brodzicka et al. (Belle Collaboration), Prog. Theor. Exp. Phys. 2012, 04D001 (2012).

[10] T. Abe et al., Prog. Theor. Exp. Phys. 2013, 03A003 (2013).

[11] M. Masuda *et al.* (Belle Collaboration), Phys. Rev. D **97**, 052003 (2018).

[12] Q. N. Xu et al. (Belle Collaboration), arXiv:1805.03044[hep-ex] (2018).